The effect of different flight heights on generated digital products: Dsm and Orthophoto

Mehmet Özgür Çelik*1, Aydın Alptekin1, Fatma Bünyan Ünel1, Lütfiye Kuşak1, Engin Kanun1

1Mersin University, Engineering Faculty, Geomatics Engineering Department, Mersin, Turkey

ABSTRACT

Unmanned Aerial Vehicle (UAV) allows you to create digital surface models (DSM) and orthophotos of an area in a short time by photogrammetric methods. In the last decade, UAV and Global Positioning System (GPS) have been used to create real, reliable and high-resolution maps. In this study, the effect of flight height on DSM and orthophoto was investigated. Two flight plans at a height of 30 to 50 meters were prepared. Images taken with UAV were used to produce DSM and orthophoto. Resolutions of maps were compared when models were produced. Compared to a flight height of 50 meters, a more detailed and high-resolution model was created with 30 meters. Although the flight data from 30 meters gave better results, the flight process took longer. Also, more photos were taken and the file size took up more space. As a result of this comparison, it was determined that the flight height should be determined according to the terrain structure, accuracy, precision and time-cost balance expected from the job.

1. INTRODUCTION

Using the unmanned aerial vehicle (UAV), flights at different heights were carried out within the same time frame. Firstly, the flights were made to be 0.82 cm/pixel GSD at a height of 30 meters and then 1.37 cm/pixel GSD at a height of 50 meters. Digital surface model (DSM) and orthophoto were produced from photos taken with UAV by photogrammetric methods. Different camera angles affect the point position accuracy and resolution of the digital products produced (Öztürk et al., 2017). To eliminate this effect, a 90-degree camera angle was used on both flights. In this study, the differences between orthophotos and DTMs with different height and ground sampling distance (GSD) were investigated. The effect of the change of GSD value on the DSM and orthophoto was investigated.

1.1. Photogrammetry

Photogrammetry is the science that enables the determination of the position, shape and size of objects on the earth utilizing overlapping pictures.

Photogrammetry with the developing technology gives faster and more accurate results compared to classical terrestrial measurements. Nowadays, air photogrammetry, which is the sub-branch of frequently preferred photogrammetry, can determine the shape, position and size of the objects in space through UAV. In this study, DSM and orthophoto were produced by using UAV. Photogrammetric methods were used to produce this data. With the development of computers, different photogrammetric approaches have started to be used for 3D model creation (Sarıtürk and Şeker, 2017). Of these, the Structure From Motion (SFM) approach is frequently preferred (Dellaert et al., 2000; Furukawa and Hernández, 2013; Sarıtürk and Şeker, 2017). SFM; 3D modelling is a classical photogrammetry approach that uses the stereo image technique to produce the model by detecting the common points of the desired object in the captured images (Dellaert et al., 2000; Furukawa and Hernández, 2013; Yakar and Doğan, 2017). The SFM enables 3D models to be produced from 2D images shot sequentially. It also enables low-cost operation with high resolution and large data sets. (Kolzenburg et al., 2016; Morgan and Brogan, 2016;

* Corresponding Author

*(mozgurcelik@mersin.edu.tr) ORCID ID 0000 – 0003 – 4569 888X
(aydinalptekin@mersin.edu.tr) ORCID ID 0000-0002-5605- 0758
(fatmabunel@mersin.edu.tr) ORCID ID 0000-0002-9949-640X
(lutfiyekusak@mersin.edu.tr) ORCID ID 0000- 0002-7265 – 245X
(ekanun@mersin.edu.tr) ORCID ID 0000-0002-2369-5322
DOI: XXXXXXXXXXXX /Research Article

Sarıtürk and Şeker, 2017). Therefore, the main purpose of this approach is to create a 3D visualization rather than a map (Seren and Demirel, 2016). The 3D model obtained by photogrammetry technique is a reference point that will facilitate the decision-making process of managers (Şasi and Yakar, 2018). In this study, DSM and orthophoto images of the study area were produced with Agisoft Metashape Professional.1.5.0 program which uses the SFM algorithm (Fig.1, Fig.2).
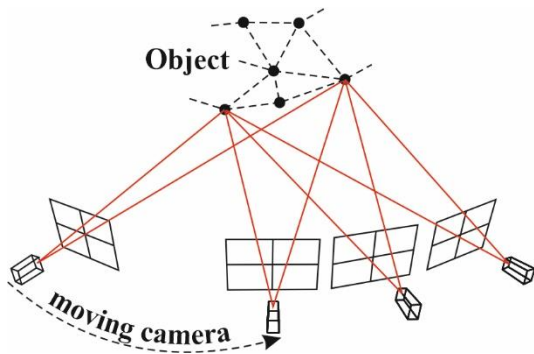

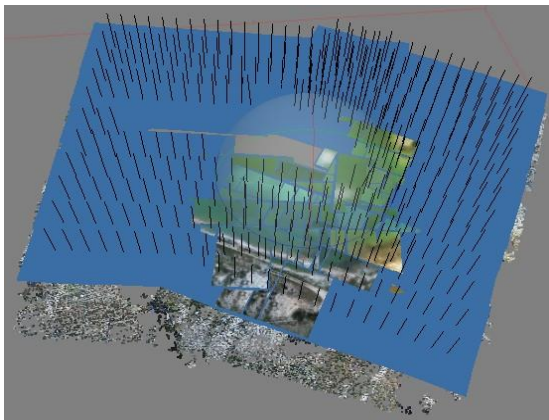**Figure 1.** Structure From Motion (It was adjusted from (Sweeney, 2016))

Figure 2. Sturucture From Motion (SFM) for Agisoft

1.2. Unmanned Aerial Vehicle (UAV)

UAV is a concept that emerged in the 70s (Newhall, 1969; Whittlesley, 1970). With advancing technology, helicopters, aircraft, rotary/fixed-wing UAVs were produced (Özemir and Uzar, 2016). UAV has contributed significantly to the process of making various maps for analysis, inquiry, 3D modelling and digital imaging (Özemir and Uzar, 2016; Nex and Remondino, 2013). The UAV is the remote control or the vehicle flying according to a flight plan (Eisenbeiss, 2009; Ceylan et al, 2014). UAV consists of a digital camera and GPS integration (Eisenbeiss, 2003; Yılmaz et al., 2018). Compared to other aircraft, the main difference is that there is no physical pilot (Eisenbeiss, 2004; Rawat and Lawrence, 2014). It is used in many fields such as

cartography, military activities, agricultural studies, and engineering projects (Fig.3).

Figure 3. UAV

1.3. UAV Benefits

UAVs have high performance at low cost. It is integrated with various imaging devices with sensors such as thermal, infrared, hyper spectral, radar, chemical and biological. There are many advantages such as providing natural disasters to ground stations, coordinating the data instantly thanks to being integrated with GPS (Yılmaz et al., 2018). It also offers the opportunity to work in risky and inaccessible areas (Ulvi and Toprak, 2016). In addition to these advantages, it is used in mapping and architectural applications and in archaeological sites (Ulvi and Toprak, 2016).

In this study, ıt was used in order to produce precision, reliable and rapid production of the field's DSM and orthophoto.

1.4. Land Models

Land models are created to obtain reliable and accurate information on topography. The terrain models are basically expressed in three ways (Fig.4).
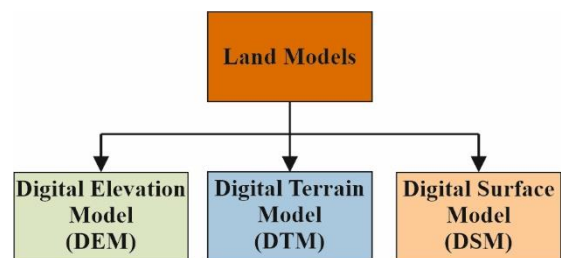

Figure. 4. Land Models

DEM: X, Y and Z (Marangoz, 2014) is the model that expresses the soil most simply and barely with height values. Various remote sensing and photogrammetric (stereo photogrammetry (Hohle, 2009; Kraus, 2007), satellite and radar images, interferometry (Arun, 2013), airborne laser

scanning (Vosselman and Maas, 2010) and land surveying (Wilson and Gallant, 2000) methods are used to obtain DEM. The method used directly affects the accuracy, cost and duration of the DEMs produced.

DTM: It is the model that includes only the bare land surface and the morphology of the land where details such as vegetation, tree, lamppost and building are not shown (ATLIS Geomatics 2019; Yasayan, 2011; Marangoz, 2014).

DSM: It is a terrain model similar to DEM and DTM. The main difference includes building, tree, tower, pole and details. In other words, it is the model that includes the height of the detail in the field.

In this study, the flights were performed two different heights (30 and 50 m) with UAV. Using the SFM approach, DEM, orthophotos and DSMs were produced from DEM. The effect of altitude and correspondingly changing GSD values on DSM and orthophoto were investigated.

GSD: The distance between the centers of two neighboring pixels in a digital image or orthophoto is called the GSD. In other words, it is the value that indicates how much area or detail a pixel represents in the field. For example, in this study, GSD is 0.82 cm/pixel for the flight that performed 30 m height. This means that details less than 0.82 cm in the field are not shown on the map.

1.5. Global Navigation Satellite System (GNSS)

GNSS is a system for determining the position of any object in the world with radio signals (Fig.5). In this study, it was used to determine the coordinates of the ground control points established before the flight with UAV. The coordinated photographs are coordinated with the photographs obtained from the flights performed at different heights (30 m and 50 m).

Figure 5. GNSS and receiver

2. STUDY AREA

The study area was determined in Aydınlar Pond located in Avgadı Neighborhood of Erdemli district of Mersin. Aydınlar Pond, which is the

working area, is located 35.5 km from Erdemli district and 90.3 km from Mersin city centre (Fig.6). The size of the area is approximately 15224.94 m^2.
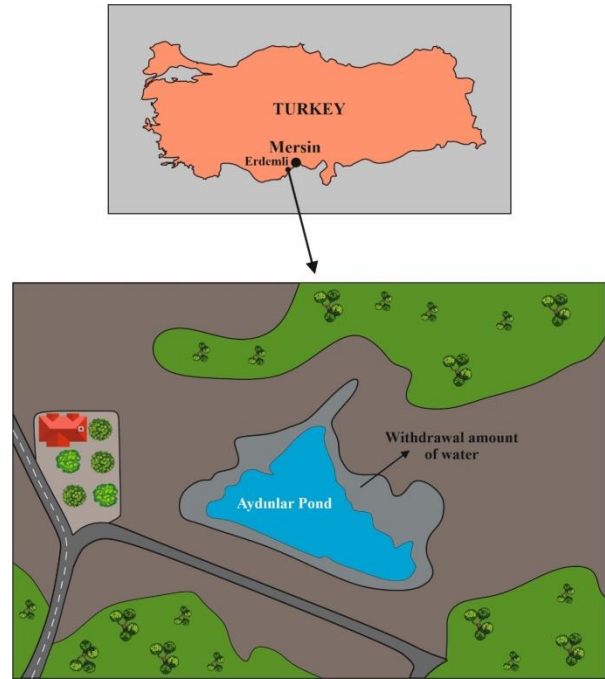

Figure 6. Aydınlar Pond

3. MATERIAL AND METHODS

3.1. Flight Planning

Flight plans were prepared in Pix4Dcapture application in the study area. For a flight at a height of 30 m, GSD is 0.82 cm/pixel (Fig.7) and for a 50 m height, GSD is 1.37 cm/pixel (Fig.8). The transverse and longitudinal overlap is set at 80% in flight plans. The camera angle is set to 90 degrees. In this study, it is planned to determine the effect of different heights on the DSM and orthophoto. Therefore, the camera angle was adjusted to 90 degrees on both flights and the angle effect was eliminated.

Figure 7. Flight plan for a height of 30 m

Figure 8. Flight plan for a height of 50 m

3.2. Field Study

3.2.1. Measurement of Gcp

5 gcps was installed to cover the area (Fig.9). The coordinates of the gcps were measured to TUSAGA Active CORS-TR system with Satlab SL800 GNSS receiver in UTM projection, ITRF-96 datum (EPSG: 5255), GRS80 ellipsoid, 2005.0 epoch, 3 degree zone 33 (Fig.10).

Figure 9. Gcp marking

Figure 10. Gcp measurement

The coordinate values of the measured gcps are shown in table 1 and table 2.

Table 1. Gcp coordinate value

Point No	Uncertainty Solution Status	Antenna Height	Accuracy Coordinate (ITRF -TM 3° 33° E)	
			Y	X
1	FIXED*	2.000	600611.675	4072972.269
2	FIXED	2.000	600649.172	4072956.432
3	FIXED	2.000	600695.871	4072941.124
4	FIXED	2.000	600768.877	4072931.886
5	FIXED	2.000	600772.124	4073008.920

Table 2. Gcp coordinate value

Point No	Ellipsoid height (h)	Orthometric height (H)
1	1401.586	1371.871
2	1401.422	1371.710
3	1400.809	1371.101
4	1400.103	1370.399
5	1399.614	1369.903

3.2.2. Taking Photos

450 photographs were taken on 30 m high flight and 259 photographs were taken on 50 m high flight. The 21 MP camera on the Parrot Anafi UAV was used. Photographs of the entire study area were taken at regular intervals (Figure.11, Figure.12).
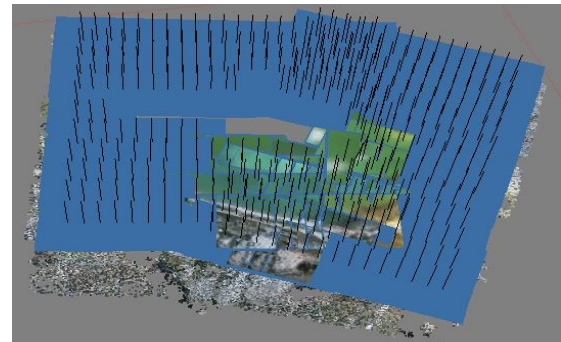

Figure 11. Photos taken at a height of 30 m

Figure 12. Photos taken at a height of 30 m

The table 3 shows the technical specifications of the Parrot Anafi UAV.

Table 3. Technical specifications of the Parrot Anafi UAV (Parrot, 2018)

Property	Value
Drone weight	320 g
Controller weight	386 g
Battery weight	126 g
Max. flight time	25 min
Max. horizontal speed	15.2 m /s
Max. vertical speed	4 m/s
Max. wind resistance	13.9 m/s
Max. transmission range	4000 m
Max. altitude	150 m
Operating temperature range	-10-40 C°
Camera	21 MP
Resolution	4608x3456
Focal length	4 mm
Pixel size	1.34 x 1.34 μm

3.3. Data Processing

With the photographs taken, Agisoft. Metashape Professional.1.5.0 program was used. The photographs were directed in the program. The estimated shape of the 3D model was generated by a sparse point cloud. All photos containing the images were matched. Internal matching elements, camera calibration information and distortion errors were calculated by this matching process.

Table 4. Calibration coefficients and correlation matrix for 30 m

	Value	Error	F	Cx	Cy	B1	B2	K1	K2	K3	P1	P2
F	3057.11	1.5	1.00	-0.74	-0.03	-0.01	-0.03	-0.13	0.36	-0.49	0.69	0.11
Cx	22.0817	0.047		1.00	0.13	0.02	0.12	0.12	-0.27	0.36	-0.31	-0.05
Cy	3.27805	0.026			1.00	-0.11	0.01	0.01	-0.02	0.03	0.00	0.50
B1	-7.05016	0.019				1.00	-0.03	-0.01	-0.01	0.01	0.01	-0.07
B2	-0.0193734	0.021					1.00	0.02	-0.00	0.01	0.02	0.07
K1	-0.00370674	2.6e-005						1.00	-0.87	0.78	-0.09	-0.02
K2	0.0128301	7e-005							1.00	-0.97	0.22	0.05
K3	-0.00986092	6e-005								1.00	-0.31	-0.06
P1	0.00374189	2.7e-006									1.00	0.08
P2	0.000525402	2e-006										1.00

Table 5. Calibration coefficients and correlation matrix for 50 m

	Value	Error	F	Cx	Cy	B1	B2	K1	K2	K3	P1	P2
F	3031.44	1.2	1.00	-0.85	-0.84	-0.06	-0.04	-0.16	0.42	-0.54	0.70	0.06
Cx	23.1364	0.049		1.00	0.73	0.06	0.16	0.14	-0.36	0.46	-0.44	-0.03
Cy	2.59885	0.042			1.00	-0.10	0.05	0.13	-0.36	0.46	-0.58	0.19
B1	-4.0701	0.044				1.00	-0.00	0.00	-0.02	0.02	-0.03	-0.01
B2	0.328655	0.043					1.00	0.01	-0.01	0.02	-0.03	-0.03
K1	-0.00407434	2.1e-005						1.00	-0.79	0.71	-0.12	-0.05
K2	0.0142818	5.4e-005							1.00	-0.98	0.24	0.01
K3	-0.0104624	4.7e-005								1.00	-0.33	-0.01
P1	0.00368191	2.1e-006									1.00	0.08
P2	0.000513487	1.4e-006										1.00

Then, a dense point cloud was formed. DEMs and DSMs were generated from dense point clouds

(Fig.13, Fig.14) produced. Orthophoto (Fig.15, Fig.16) were generated from DEM.
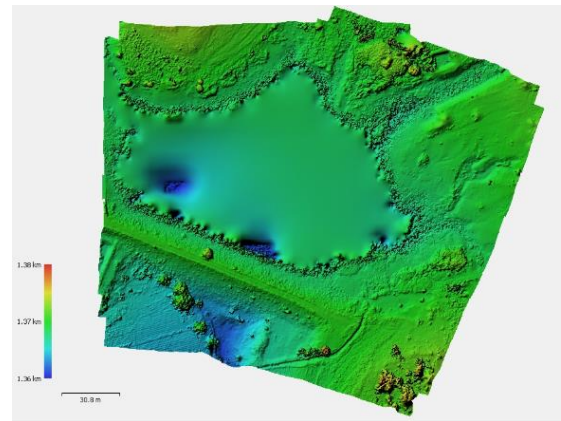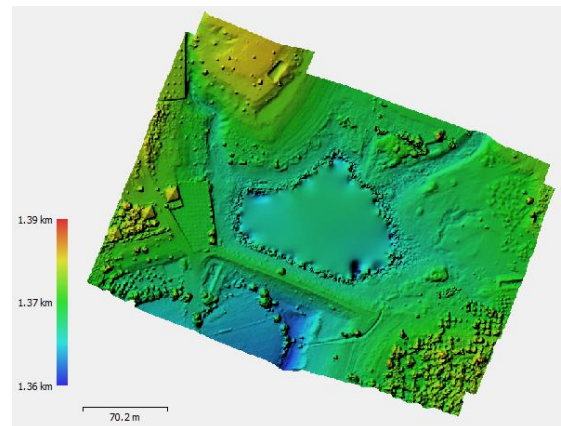

Figure 13. DSM for 30 meters.
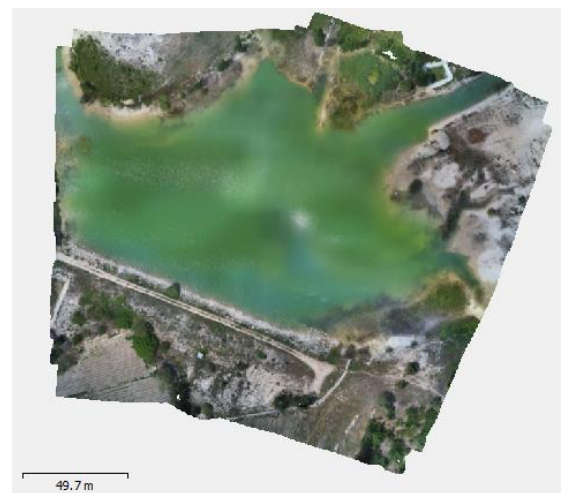

Figure 14. DSM for 50 meters.

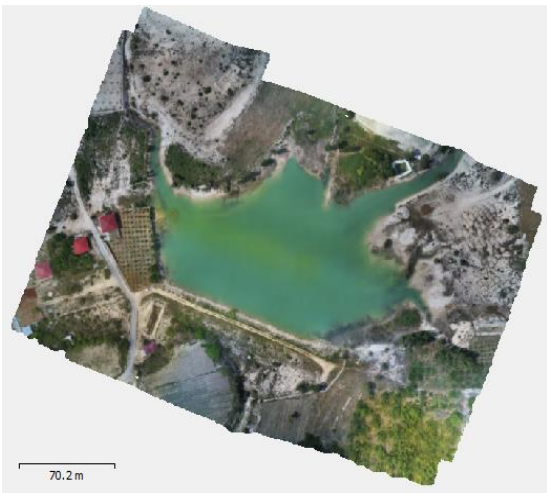**Figure 15.** Orthophoto for 30 meters

Figure 16. Orthophoto for 50 meters

The process steps performed during the study are shown in the following figure (Fig. 17).
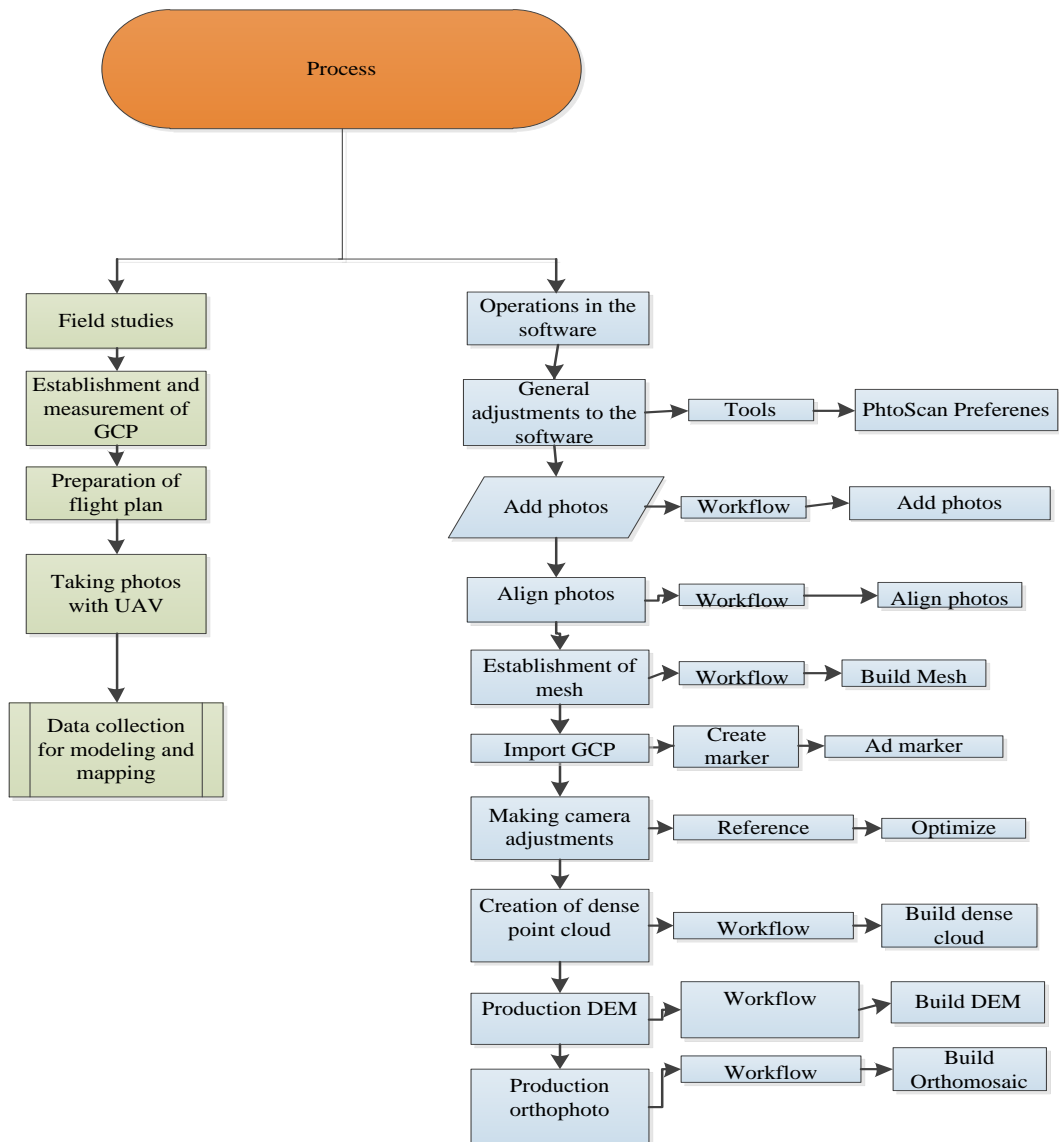

Figure 17. Work flow

4. FINDINGS

In the study conducted in a flight from a height of 30 m DSMGSD: 4.24cm/pixel, orthophotoGSD: 1.09 cm/pixel. In the 50 m flight, DSMGSD is 6.78 cm/pixel and orthophotoGSD is 1.74 cm/pixel. Based on these data, it was determined that flight height directly affected the resolution of digital products (such as DSM, orthophoto) depending on the terrain structure, desired accuracy and sensitivity (Fig.18, Fig.19). To obtain more detailed and reliable information about the terrain, it has been determined that low altitude flights should be performed. Although UAVs have many advantages, they have been determined as a result of the wind which is effective during the field study, including the shortness of time in the air and the inability to work optimally in windy weather.

Figure 18. An image from a 30 meters flight

Figure 19. An image from a 50 meters flight

5. CONCLUSION

As a result of the study, it was found that high accuracy and precision data can be obtained with

UAV and digital products of unreachable areas can be created. It has been determined that with UAV, operations can be performed in a shorter time compared to terrestrial measurements. In addition, the use of UAV has been seen to beneficial for users in terms of cost and accuracy (Akar, 2017).

The output products obtained as a result of the study DSM and orthophoto images; Horizontal position error for flight at 30 m height: ± 1.30 cm, vertical position error: ± 0.32 cm, total error: ± 1.34 cm was determined. For the flight at 50 m height, horizontal position error: ± 3.80 cm, vertical position error: ± 0.56 cm, total error: ± 3.84 cm was determined. It was seen that point position accuracy is higher at 30 m flight height.. Different camera angles affect point position accuracy and resolution (Öztürk et al., 2017). In order to eliminate this effect, flights were performed with a 90-degree camera angle.

It has been determined that flight height directly affects the resolution of the output products to be obtained. Geomorphological structure of the study area, land use method, flight altitude should be changed depending on the accuracy and sensitivity expected from the work.

NOTE: This study is an extended version of the paper presented at the CISET 2019 Symposium held between 10-12 October 2019 at Mersin University.

REFERENCES

Akar, A . (2017). "Evaluation of Accuracy of Dems Obtained From Uav-Point Clouds for Different Topographical Areas." International Journal of Engineering and Geosciences, 2(3), 110-117. doi: 10.26833/ijeg.329717

ATLIS Geomatics, http://www.atlisgeo.com/expertise/process/dem-dtm/ [Accessed 17 Oct. 2019].

Arun, P.V. (2013). "A comparative analysis of different DEM interpolation methods." Geodesy and Cartography, 39 (4), 171-177.

Ceylan, M., Doner, F., & Ozdemir, S. (2014). "Use of unmanned aerial vehicle systems in data collection and mapping studies." 5. Remote Sensing-GIS symposium, Istanbul, Turkey.

Dellaert, F. Seitz, S. M., Thorpe, C. E., & Thrun, S. (2000). "Structure from motion without correspondence. Proceedings." IEEE Conference on Computer Vision and Pattern Recognition, CVPR 2000 (Cat. No.PR00662), Hilton Head Island, SC, 557-564 Vol. 2, doi: 10.1109/CVPR.2000.854916.

Eisenbeiss, H. (2003). "Positions und orientierungsbestimmung eines autonomen helikopters-vergleich zwischen direkter

georeferenzierung und aerotriangulation mit videobilddaten." Diploma Thesis, Institute for Photogrammetry and remote sensing, University of Technology, Dresden, Germany.

Eisenbeiss, H. (2004) "A mini unmanned aerial vehicle (UAV): system overview and image acquisition." International Archives of Photogrammetry, Remote Sensing and Spatial Information Sciences, vol. 36, part 5/W1, on CD-ROM.

Eisenbeiss, H. (2009). UAV Photogrammetry, ETH Zurich for the degree of Doctor of Science, ISNN 0252-9335, ISBN: 978-3-906467-86-3, Zurich, Switzerland.

Furukawa, Y., and Hernández, C. (2013). "Multi-View Stereo: A Tutorial." Foundations and Trends® in Computer Graphics and Vision, Vol. 9, No. 1-2, 1-148.

Hohle, J. (2009). "DEM generation using a digital large format frame camera." Photogrammetric Engineering and Remote Sensing, 75 (1), 87–93.

Kraus, K. (2007). "Photogrammetry, Geometry from Images and Laser Scans (2nd edition)" Walter de Gruyter, Berlin, Germany, 459.

Kolzenburg, S., Favalli, M., Fornaciai, A., Isola, I., Harris, A. J. L., Nannipieri, L., & Giordano, D. (2016). "Rapid updating and improvement of airborne lidar DEMs through ground-based sfm 3-d modelling of volcanic features." IEEE Transactions on Geoscience and Remote Sensing, Vol. 54, No. 11, 6687-6699.

Marangoz, A., M. (2014). "Lecture notes on photogrammetry II". Bülent Ecevit University, Zonguldak, Turkey.

Morgan, J. A., and Brogan, D. J. (2016). "How to Visual SFM". Department of Civil & Environmental Engineering Colorado State University Fort Collins, Colorado.

Newhall, B. (1969). "Airborne camera: The world from the air and outer space." Hasting House Trowbridge&London, 144.

Nex, F., and Remondino, F. (2014). "UAV for 3D mapping applications: a review." Applied Geomatics, Vol. 6, Issue 1, 1-15.

Özemir, I., and Uzar, M. (2016). "The generation of photogrammetric data with unmanned aerial vehicle." 6. Remote Sensing-GIS Symposium, Adana, Turkey, 245-254.

Öztürk, O., Bilgilioğlu, B., Çelik, M., Bilgilioğlu, S, & Uluğ, R . (2017). "Investigation of the Effect of Height and Camera Angle on Accuracy in Orthophoto Production with Unmanned Aircraft (UAV) Images." Geomatik, 2(3), pp. 135-142. doi: 10.29128/Geomatik.327049.

Parrot (2018) "Anafi User Manual v2.2." pp.1-73.

Rawat K. S., and Lawrence E. E. (2014). "A mini-UAV VTOL Platform for Surveying Applications." International Journal of Robotics and Automation (IJRA) Vol. 3, No. 4, 259-267.

Sarıtürk, B., and Şeker D.Z. (2017) "Comparison Of Commercial And Open-Source Software Used In 3d Object Modeling With Sfm Technique." Afyon Kocatepe University Journal of Science and Engineering, Special Issue, 126-131.

Şasi, A., and Yakar, M. (2018). "Photogrammetric Modelling Of Hasbey Dar'ülhuffaz (Masjid) Using An Unmanned Aerial Vehicle." International Journal of Engineering and Geosciences, 3(1), 6-11. doi: 10.26833/ijeg.328919

Seren, A. M., and Demirel, H. (2016). "3 Dımensıonal Modellıng of Large Objects in Open-Space: A Comparıson of Recent Methodologıes in Geomatıcs Engıneerıng." 8. National Engineering Surveys Symposium, Yıldız Technical University, Istanbul, Turkey.

Sweeney, C. (2016). Theia Visison Library http://www.theia-sfm.org/sfm.html [Accessed 11 Oct. 2019].

Ulvi, A., and Toprak, A.S. (2016). "Investigation Of Three-Dimensional Modelling Availability Taken Photograph Of The Unmanned Aerial Vehicle; Sample Of Kanlidivane Church." International Journal Of Engineering and Geosciences, 1(1), 1-7. doi: 10.26833/ijeg.285216.

Vosselman, G., and Maas, H.G. (2010). "Airborne and Terrestrial Laser Scanning." CRC: Boca Raton, FL, USA, 318.

Whittlesley, J. H. (1970). "Tethered Balloon for Archaeloogical Photos, In Photogrammetric Engineering." 36 2, 181-186.

Wilson, J.P., and Gallant, J.C. (2000). Secondary Topographic Attribute. in: Wilson, J.P., and Gallant, J.C. (Eds.), "Terrain Analysis: Principles and Applications."

John Wiley, and Sons., New York, 87–131.

Yılmaz, H. M., Mutluoglu, O., Ulvi, A., Yaman, A., & Bilgilioglu, S. S. (2018). "Created Tree Dimensional Model of Aksaray University Campus with Unmanned Aerial Vehicle." Journal of Geomatics, No. 2018; 3(2), 129-136.

Yakar, M., and Dogan, Y. (2017). "3D Modelling of Silifke Asagi Dunya Sinkhole by Using UAV." Afyon Kocatepe University Journal of Science and Engineering, Special Issue, 94-101.

Yasayan, A. (2011). "Photogrammetry." T.C. Anatolia University Publications, No. 2295. Open Education Faculty Publication No: 1292, Eskisehir, Turkey.